Smart Structures and Systems, *Vol. 29, No. 3 (2022) 485-498*
https://doi.org/10.12989/sss.2022.29.3.485

Hysteretic model of isolator gap damper system and its equivalent linearization for random earthquake response analysis

Hongmei Zhang* and Chen Gu [a]

College of Civil Engineering and Architecture, Zhejiang University, Hangzhou, 310058, China

(*Received June 28, 2021, Revised December 9, 2021, Accepted December 17, 2021*)

Abstract. In near-fault earthquake prone areas, the velocity pulse-like seismic waves often results in excessive horizontal displacement for structures, which may result in severe structural failure during large or near-fault earthquakes. The recently developed isolator-gap damper (IGD) systems provide a solution for the large horizontal displacement of long period base-isolated structures. However, the hysteresis characteristics of the IGD system are significantly different from the traditional hysteretic behavior. At present, the hysteretic behavior is difficult to be reflected in the structural analysis and performance evaluation especially under random earthquake excitations for lacking of effective analysis models which prevent the application of this kind of IGD system. In this paper, we propose a mathematical hysteretic model for the IGD system that presents its nonlinear hysteretic characteristics. The equivalent linearization is conducted on this nonlinear model, which requires the variances of the IGD responses. The covariance matrix for the responses of the structure and the IGD system is obtained for random earthquake excitations represented by the Kanai-Tajimi spectrum by solving the Lyapunov equation. The responses obtained by the equivalent linearization are verified in comparison with the nonlinear responses by the Monte Carlo simulation (MCS) analysis for random earthquake excitations.

Keywords: gap damper; IGD system; isolator-gap damper; Lyapunov equation; Monte Carlo simulation; stochastic equivalent linearization

1. Introduction

Base isolation is one of the effective methods to mitigate structural vibration from extreme seismic activity (Li and Li 2019). In 1970, the concept of seismic base isolation was first proposed in New Zealand. Then, the first base-isolated building was built in Japan. After that, from 1985 to 1994, about 10 base-isolated buildings were built in Japan each year (Pan *et al*. 2005). The rapid implementation of such buildings promoted the development of the various design and evaluation methods (Nakashima and Bruneau 1995, Kishida *et al*. 2017). Although the base isolators showed excellent vibration mitigation effect in low-level or design earthquakes (Sato *et al*. 2011), they produced excessive displacement; this lead to large pulse-like ground motions generated at the near-fault location (Kelly 1999, Farsangi *et al*. 2018). It was also found to pound between the structure and the moat wall and then increased the acceleration of the superstructure in the case of extreme events (Zargar *et al*. 2013).

To limit the extreme displacement of the isolator, the isolation system designer combines displacement-dependent dampers with isolators. Zargar *et al*. (2013) connected a damper to the isolator by a contact rigid block with certain gap and that was experimentally demonstrated with significantly reduced the risk of collapses of the isolator structures. De Domenico *et al*. (2020a) numerically verified the proposed base-isolation system with initial gap efficiently combines satisfactory energy dissipation, which reduces the displacement demand. This hybrid base-isolating system composed the pure isolators composed of natural rubber bearings, high damping rubber bearings, lead rubber bearings, and sliding bearings (Tu *et al*. 2009) with supplemental dampers such as viscos, hysteretic or friction dampers. In that system, the restoring force is mainly provided by the isolators, and the initial gap is result in a low residual displacement of the structure (De Domenico *et al*. 2020a).

The gap element and energy dissipation device are often included in a gap damper; the gap damper can only be activated when the displacement of the isolator reaches a certain limit value, and it then provides the extra energy dissipation capacity for the system. This characteristic of the gap dampers can limit the lateral displacement within the isolator level and protect the structures from collapse in cases of extreme earthquakes.

After the gap damper device was proposed, estimation models of gap dampers were developed; this provided an evaluation measure for the effectiveness of the gap damper models using the predictive index, and the differences between various models were compared (Zargar *et al*. 2013). The effectiveness of reducing the displacement for the IGD was experimentally verified for both whole and local aspects (Rawlinson *et al*. 2015, Zargar *et al*. 2017). The structural floor acceleration due to excessive damping

*Corresponding author, Associate Professor,
E-mail: zhanghongmei@zju.edu.cn
[a] Graduate Student, E-mail: guchen@zju.edu.cn

ISSN: 1738-1584 (Print), 1738-1991 (Online)

and possible pounding was analyzed (Kelly 1999). The demand for application promotes the design innovation of IGDs. De Domenico *et al*. (2020a, b) studied the effectiveness of combining low-friction curved surface sliders and hysteretic gap dampers and presented a base isolation layout with shape memory alloy gap dampers. Han *et al*. (Han *et al*. 2005, 2007, 2008) proposed a soft collision scheme using a rigid coil spring stopper and a composite stopper; they conducted experiments under reserved load on the damping characteristics of the stopper. Yang *et al*. (2019) used a mild steel limit device as flexible buffer for the structure in a space at a certain height of the base isolation layer. Zhao *et al*. (2013) applied the reinforced concrete short column to the hysteresis-friction parallel isolation system and determined the buffer limit distance to the reinforced concrete short column. Xiong *et al*. (2008) used the mild steel U-shaped belt piece as the limit energy dissipation element; they calculated the length of the slip zone between the foundation and the limit energy dissipation device, which overcame the previous drawback. Liu *et al*. (2018) also set a certain length for the sliding zone of the proposed new limit device.

Based on experimental verifications, the gap dampers are expected to have a significant positive effect on the structures in the near-fault area. Since the hysteretic behavior of the IGD system includes a gap phase combined with hysteretic characteristics of an isolator, it is difficult to conduct effective simulation. The existing numerical evaluation methods still lack effectiveness for the significant characteristics of the hysteretic curve that is rather complex in the nonlinear behavior. Although the IGD system is assumed as a multifunctional seismic mitigation method especially in near fault area, the lack of effective models for evaluating the nonlinear hysteretic behavior may lead to the improper design and application of this kind of IGD system, which may result in serious structural failure during large or near-fault earthquake. And more importantly, the nonlinear response of the IGD system during earthquake events are hardly to be evaluated, particularly for the potential serious structural failure under extreme earthquake.

The nonlinear response for random excitations statistically provides structural responses, which can provide an important structural seismic parameter optimization design method for this kind of structures in view of probability. Methods for the analysis of nonlinear systems under random excitation (such as Markov method and equivalent linearization method) are a more general way to evaluate the seismic performance of structures (Roberts 1981a, b). Among those methods, the equivalent linearization method is widely used in practical engineering problems. It has been successfully applied to hysteretic systems in the stationary process (Lei and Qiu 1997) by using the Lyapunov equation to solve the covariance matrix of the response (Soong and Grigoriu 1993). Then, researchers extended it to the system subjected random ground motion to obtain the effective response covariance matrix (Xu *et al*. 2017, Crandall and Mark 1963). Yan and Nie (2000) evaluated the nonlinear response of the simplified flag shaped (SFS) model, and Zhang *et al*. (2020) evaluated the nonlinear response of the modified flag shaped (MFS) model.

The purpose of this study is to provide a response evaluation model to a structure with an IGD system, which can be used for the nonlinear response evaluation under random earthquakes. Three parts of the IGD model (IGDM) are proposed using mathematical expressions to represent the hysteretic characteristics of the IGD system. They include a linear elastic part and two hysteretic parts, and the corresponding equivalent linearization coefficients are obtained. A SDOF structure with an IGD system of various initial gaps a, energy dissipation coefficients of the isolator, λ_1, and energy dissipation coefficients of gap damper, λ_2 is analyzed under random seismic excitations. To obtain the response of the structure after the equivalent linearization of the IGDM, the Lyapunov equation is employed. The simulated responses via Monte Carlo method are used as the actual responses and compared with those by the equivalent linearization. The proposed mathematic expression and the equivalent linearization were validated by the MCS for a SDOF structure with various design parameters of the IGD (Gazi and Alhan 2018). This research has important significance for the seismic performance evaluation for the near-fault buildings with an IGD system by providing an effective mathematical method for random earthquake excitations. It also can be used as a theoretical guidance for the future application and development of the optimal IGD system.

2. Proposed IGD model (IGDM)

2.1 Description of gap damper system

A gap damper is a passive control device, which can provide phasic energy dissipation function. It is not activated during medium and small earthquakes. During a extreme earthquake, when the isolator displacement reaches the initial gap, the gap damper is triggered to increase damping and control the displacement as Fig. 1 shows. The purpose is to prevent the structure from extreme displacement which may cause catastrophic collapse. Generally, the gap dampers can be hysteretic gap dampers, friction dampers and viscous gap dampers. The Kelvin gap damper, two-phase viscoelastic gap damper, and two-phase viscous plastic gap damper (Zargar *et al*. 2013) have been basically evolved from the hysteretic and viscous gap dampers. One end of the damper can either be fixed to the foundation or to a moat wall; the other end is fixed to the gap element. If it is fixed to the moat wall, the gap damper will only be activated in one direction; large later displacement may lead to the failure of the gap damper (Rawlinson *et al*. 2015). Hence, the energy dissipation device is usually fixed on the foundation as demonstrated in Fig. 2. Consisted by isolator, damper and gap, the IGD system can be illustrated as the schematic in Fig. 3. Within that, the isolator can mitigate the vibration of the structure and the gap damper can increase the energy dissipation capacity during extreme event, which can be a viscos damper or displacement dependent damper. The hysteresis

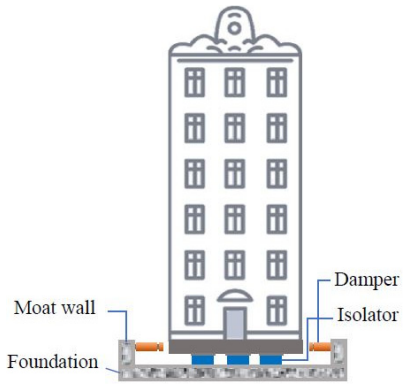

Fig. 1 Diagram of a structure with IGD

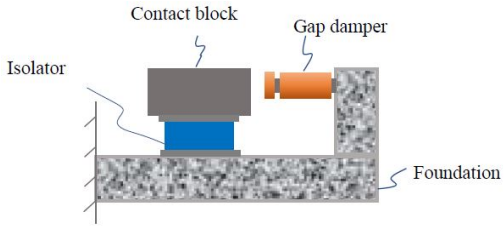

Fig. 2 IGD connected with foundation

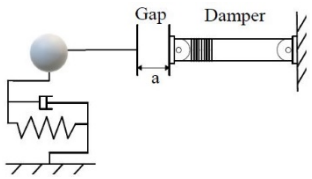

Fig. 3 Schematic of an IGD system with a rigid mass

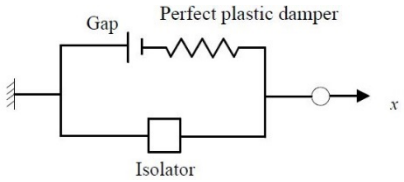

Fig. 4 Mechanical model of IGD system with hysteretic gap damper

curve formed by the viscous gap damper is complex to express mathematically. So, in this study, the gap damper is adopted as a kind of perfectly plastic damper with a certain initial gap as in Fig. 4. Self-centering dampers is important for the functional maintenance structure beside the seismic energy dissipation capacity (Zhang *et al*. 2022). In the IGD system, the gap damper is also intended to be designed with self-restoring capacity to return to the initial position. Zargar investigated the impact of the residual deformation to the system response, and that indicates the reserved gap changes that will lead to a reduction in the overall performance of the gap damper by no more than 10% to limit isolator displacement and roof acceleration (Zargar *et al*. 2013). The system restoring force can be provided by isolators with high re-centering capability, and the IGD system results in negligible residual displacements (De Domenico *et al*. 2020a).

2.2 Mechanical behavior of IGD system

The IGD is usually fixed between the structure and the foundation. Thus, when the bottom layer of the structure is displaced, the isolation nub is also displaced. When the structure is exposed to small and medium earthquakes, the displacement of the isolation nub does not exceed the initial gap to trigger the damper to increase damping. However, when the structure is exposed to extreme earthquakes, such as near-fault motion, the displacement of the isolation nub may be larger than the initial gap, and the damper is triggered. In the process of pushing and pulling, the damper produces damping to control the isolator displacement. In this paper, the hysteresis model of the IGD is divided into three parts as in Fig. 5. The isolator consumes energy while the gap damper has not been activated, in which, the hysteric behavior can be divided as elastic line and a pure energy dissipation part as in Figs. 5(a) and (b) shows. When the gap damper is triggered, because the yield displacement of the hysteretic gap damper is very small (De Domenico *et al*. 2020a), the diagonal line segment is simplified to a straight-line segment perpendicular to the x-axis for convenience of mathematical expression. In terms of material, when the displacement of the isolator reaches the initial gap, the external force is large enough to reach the yield strength of the elastic-perfectly plastic damper; hence, the elastic part of the elastic-perfectly plastic spring is directly completed and enters the plastic stage as shown in Fig. 5(c).

2.3 The IGD model (IGDM)

The IGDM is proposed to describe the hysteretic behavior of the IGD system. This hysteretic model curve can be divided into three parts: a linear elastic part and two hysteretic parts (Fig. 5). The linear elastic part I in Fig. 5(a) presents the stiffness of the isolator, which does not consume energy because it is a straight-line segment. Part II in Fig. 5(b) presents the hysteresis curve that is formed by the isolator, and part III in Fig. 5(c) is the simplified hysteresis curve that is formed after the gap damper is activated. Because the gap damper is not activated at the beginning to produce damping, the hysteresis curve that is formed by the gap damper is different from that of the traditional damper, which is an advantage of the gap damper. The mathematical expression of the restoring force of the IGDM can be presented as

$$g(x,\dot{x}) = k_1 x + F_1 + F_2 \tag{1}$$

$$F_1 = b\,sign(\dot{x}) \tag{2}$$

$$F_2 = \left(\frac{sign(|x|-a)+1}{2}\right)\left(\frac{sign(x)+sign(\dot{x})}{2}\right)c \tag{3}$$

where x is the displacement of the IGD, $\dot{x}$ is the velocity, k_1 is the initial stiffness, b is the damping force produced by the base isolator, and the magnitude of b is dependent on the characteristics of the isolator itself; a is the initial gap,

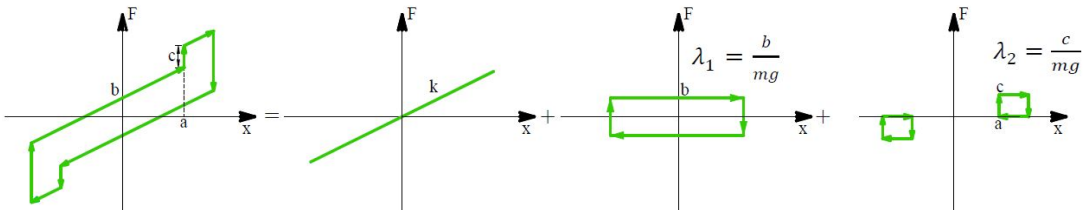

(a) (b) (c)

Fig. 5 The proposed IGD model

which refers to the distance between the isolator nub and the bumper. When the displacement of the isolator reaches a certain value, the gap damper is activated to increase damping. *c* is the added damping force after the activation of the gap damper. Different types of gap dampers correspond to different *c* values. The damper force is taken as a constant value that is independent of displacement or velocity.

3. Stochastic equivalent linearization of IGDM

3.1 Stochastic equivalent linearization

The stochastic equivalent linearization method is a generalization of the equivalent linearization method of nonlinear deterministic vibration in a stochastic process. The aim of the equivalent linearization is to minimize the mean square value of the error to determine the corresponding linear parameters (Ou and Wang 1998). The stochastic equivalent linearization method is effective for solving nonlinear random vibration problems for engineering structures. Assuming that the earthquake wave is a stationary Gaussian process, x and $\dot{x}$ are independent of each other, and they follow the Gaussian distribution. Yan and Nie (2000) proposed an equivalent linearization method for the standard flag-shape model (SFS); and Zhang *et al*. (2020) developed an equivalent linearization measure for the proposed modified flag shape (MFS) model. In the IGD system, there are residual displacement for isolator and significant sliding before the gap damper is triggered (Zargar *et al*. 2013); this is different compared to the SFS hysteretic model and MFS model. In order to analyze the stochastic response of the IGD system, an equivalent linearization method based on the above-mentioned mathematical expression for the hysteretic behavior of the IGD is proposed. Assuming the excitation is a stationary process with a zero mean x and $\dot{x}$ are also regarded as random variables with a zero mean. According to the decomposed model and the expression in Eqs. (1)-(3), the linear restoring force of the IGDM can be represented as

$$g(x,\dot{x}) = k_1 x + C_{e1}\dot{x} + k_{e2}x + C_{e2}\dot{x} \tag{4}$$

$$F_{e1} = C_{e1}\dot{x} \tag{5}$$

$$F_{e2} = C_{e2}\dot{x} + k_{e2}x \tag{6}$$

Because equivalent linearization is generally realized by minimizing the square value of the error, the necessary and sufficient conditions to reach the minimum value for E $[e^2]$ are

$$\frac{\partial E(e^2)}{\partial C_{e1}} = 0; \quad \frac{\partial E(e^2)}{\partial C_{e2}} = 0; \quad \text{and} \quad \frac{\partial E(e^2)}{\partial K_{e2}} = 0 \tag{7a}$$

where E$[e^2]$ is the expected square error from Eqs. (1) and (4), which is a random process. C_{e1} and C_{e2} are the equivalent linear damping coefficients for the dissipation system of isolator and gap damper; and k_{e1} is the equivalent linear stiffness for gap damper. Since excitation is a stationary process, Eq. (7a) can be solved as follows

$$C_{e1} = \frac{E(\dot{x}F_1)}{E(\dot{x}^2)}; \quad C_{e2} = \frac{E(\dot{x}F_2)}{E(\dot{x}^2)}; \quad \text{and} \quad k_{e2} = \frac{E(xF_2)}{E(x^2)} \tag{7b}$$

Finally, C_{e1}, C_{e2} and K_{e2} can be obtained as

$$C_{e1} = \sqrt{\frac{2}{\pi}}\frac{b}{\sigma_{\dot{x}}} \tag{8}$$

$$C_{e2} = \frac{c}{\sqrt{2\pi}\sigma_{\dot{x}}}\left(1 - erf\left(\frac{a}{\sqrt{2}\sigma_x}\right)\right) \tag{9}$$

$$k_{e2} = \frac{ce^{\frac{-a^2}{2\sigma_x^2}}}{\sqrt{2\pi}\sigma_x} \tag{10}$$

where erf(x) $= \frac{2}{\sqrt{\pi}}\int_0^x e^{-t^2}\,dt$, σ_x and $\sigma_{\dot{x}}$ are the standard deviations of x and $\dot{x}$, respectively.

3.2 Response analysis for stochastic earthquake load

With the linearized parameters, the equation of motion of the equivalent linear IGD system can be represented as

$$m\ddot{x} + k_1 x + F_{e1} + F_{e2} = -m\ddot{g}(t) \tag{11}$$

where m is the mass of the rigid structure with an IGD; x, $\dot{x}$, $\ddot{x}$ are the corresponding displacement, velocity, and acceleration of the structure as well as the IGD; k_1 is the initial stiffness of the base isolator; F_{e1} and F_{e2} are the damping forces provided by the IGD system; $\ddot{g}(t)$ is the acceleration of the ground motion. To generalize for different mass structures and to facilitate the engineering application, the expression $\frac{b}{mg}$ is represented by λ_1, and $\frac{c}{mg}$ is represented by λ_2 in this paper, which are

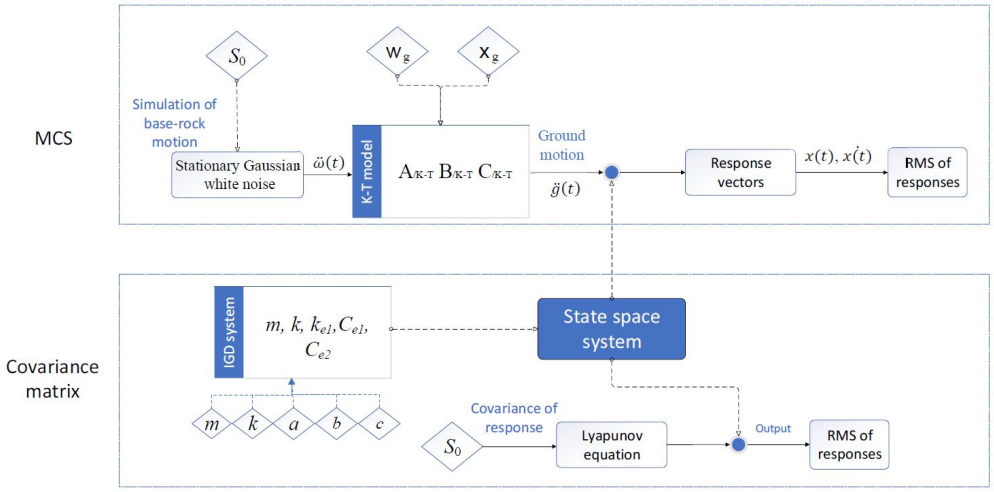

Fig. 6 Flowchart of response analysis for stochastic earthquake load

performance factors. The damping forces b and c represent the different energy dissipation capacities of isolators and gap dampers as Fig. 5 shows.

To verify the proposed mathematical expression for the hysteretic model, the nonlinear response analysis is then conducted using the Kanai–Tajimi (K–T) model (Kanai 1957, Tremblay *et al*. 2008) for the stochastic ground acceleration as follows

$$\ddot{x}_f + 2\xi_g\omega_g\dot{x}_f + {\omega_g}^2 x_f = \ddot{\omega}(t) \tag{12a}$$

$$\ddot{g}(t) = -2\xi_g\omega_g\dot{x}_f - {\omega_g}^2 x_f \tag{12b}$$

where $\ddot{\omega}(t)$ is the base rock motion, $x_f(t)$ is a system variable for the soil medium in the K–T spectrum; ω_g and ξ_g are the natural frequency and damping ratio determined by the site type. With the spectrum density S_0 and the Gaussian white noise assumption the base rock motion ($\ddot{\omega}(t)$) can be obtained as illustrated in Fig. 6. For the structural response analysis, the soil site and structure with the linearized IGD can be considered as a linear system. The state space equation can be written by combining Eqs. (11) and (12) as

$$\dot{X}_a = A_m X_a + B_m\ddot{\omega}(t) \tag{13a}$$

where $X_a = \{{X_s}^T, {X_g}^T\}^T$ is the state vector for the structure and soil site.

$$X = \{x, \dot{x}\}^T, X_g = \{x_f, \dot{x}_f\}^T \tag{13b}$$

$$A_m = \begin{bmatrix} A & BC_{K-T} \\ 0 & A_{K-T} \end{bmatrix}; B_m = \begin{bmatrix} 0 \\ B_{K-T} \end{bmatrix} \tag{13c}$$

$$A = \begin{bmatrix} 0 & 1 \\ -\dfrac{k_1 + k_{e2}}{m} & -\dfrac{C_{e1} + C_{e2}}{m} \end{bmatrix}; \quad B = \begin{bmatrix} 0 \\ 1 \end{bmatrix} \tag{13d}$$

$$A_{K-T} = \begin{bmatrix} 0 & 1 \\ -{\omega_g}^2 & -2\omega_g\xi_g \end{bmatrix}; \tag{13e}$$

$$B_{K-T} = \begin{bmatrix} 0 \\ 1 \end{bmatrix}; \qquad C_{K-T} = \begin{bmatrix} {\omega_g}^2 & 2\omega_g\xi_g \end{bmatrix} \tag{13e}$$

For a stationary earthquake excitation, the stationary Lyapunov equation can be solved for the covariance matrix (Γ_{X_a}) of X_a as

$$\dot{\Gamma_{X_a}} = A_m\Gamma_{X_a} + \Gamma_{X_a}{A_m}^T + 2\pi B_m S_0 {B_m}^T = 0 \tag{14}$$

where S_0 is the spectrum intensity of the base rock motion. When S_0 is determined, the covariance matrix of the state vector can be obtained by introducing Eq. (13) into the Lyapunov equation for Γ_{X_a}. Then the standard deviation of the state vector can be obtained from the diagonal of the covariance matrix. Because the mean value of the state vector is zero, the standard deviation can be represented as the root mean square value (RMS). The flow chart for the time history response analysis by the Monte Carlo simulation (MCS) of the ground motion and the covariance response analysis by the Lyapunov equation are illustrated in Fig. 6. More details about Eq. (14) can be found in the articles of Zhang *et al*. (2020) and Xu *et al*. (2017, 2018).

4. Verification of equivalent linearized IDGM model (EIGDM)

In this study, the MCS was used to obtain the time history response, whereas the Lyapunov equation was used to obtain the RMS responses of a rigid structure with a concentrated mass by the EIGDM. The MCS results are considered as the actual structural responses, which are used to examine the adequacy of the EIGDM.

The MCS was conducted for the nonlinear responses of the structure with an IGDM under 5000 randomly simulated earthquake waves via the Simulink module of MATLAB. To find a feasible number of the simulated earthquakes, 100 to 10000 waves with a duration of 40s were utilized in the error analysis. Fig. 7 shows the RMS of the response varying with the number of the simulated earthquakes for the IGD parameters as: a = 0.06 m, λ_1 = 0.035 and λ_2 =

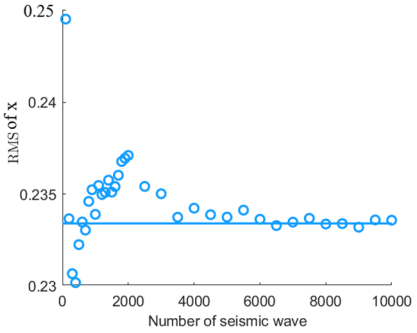

Fig. 7 RMS for different number of simulated seismic waves in MCS: Case II-1 in Table 1

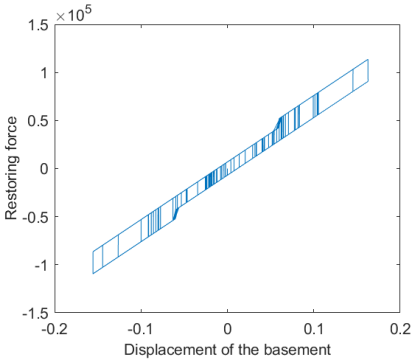

Fig. 8 Hysteretic curve of the IGD for a simulated earthquake excitation

0.04. The result indicates that the RMS is converged to a constant value when the number is over 3800. Therefore, the number of the simulated earthquakes were taken as 5000 with a duration of 40s in the following MCS analysis. The K-T spectrum were used for generating seismic waves. An earthquake event (Level 1) with an exceedance probability of 10% in 50 years in Los Angeles area was adopted in this study (Kanai 1957, Dickinson and Gavin 2010). The parameters of the K-T spectrum were taken as (Somerville *et al.* 1997) $S_0 = 0.026m^2/s^2$, $\omega_g = 4.9\,rad/s$, and $\xi_g = 1.76$. The time history responses for the structural mass were obtained using Simulink program. The EIGDM was introduced into the Lyapunov equation,

Table 1 Parameters of different IGD conditions

	Initial gap a (m)	Energy dissipation coefficient of isolator λ_1	Energy dissipation coefficient of gap damper λ_2
Case I-1	0.06	0.03	0.04
Case I-2	0.21	0.03	0.04
Case I-3	0.36	0.03	0.04
Case II-1	0.06	0.035	0.04
Case II-2	0.06	0.04	0.04
Case II-3	0.06	0.045	0.04
Case III-1	0.06	0.065	0.045
Case III-2	0.06	0.065	0.05
Case III-3	0.06	0.065	0.055

from which the covariance matrix of the responses was obtained and the RMS values were evaluated. As an example, the restoring force-lateral displacement of the IGD with parameters of a = 0.06, λ_1 = 0.08 and λ_2 = 0.07 is shown for a simulated earthquake in Fig. 8.

The proposed EIGDM was verified for various cases with different IGD parameters as shown in Table 1. The definitions of the energy dissipation coefficients (λ_1 and λ_2) are shown in Fig. 5. The IGD parameters were selected by referring the gap dampers considered for Erizcan-Turkey 1992 earthquake motion.

4.1 Different initial gaps

Figs. 12-14 present the ratios between the RMS responses using the Lyapunov equation with EIGDM and the MCS results. The IGD parameters are: a = 0.06, 0.21 and 0.36 m; whereas λ_1 = 0.03 and λ_2 = 0.04. The circles (MCS-s) are the time-varying standard deviation (RMS) of the responses obtained at different time via MCS. The straight line (MCS-t) represents the converged values of MCS-s at t = 40 s, which can be considered as the exact response. The dotted line and straight line are the results of the EIGDM obtained by the Lyapunov equation and the MCS, respectively. Compared with the responses of MCS-t, the results by the EIGDM show fairly good agreement,

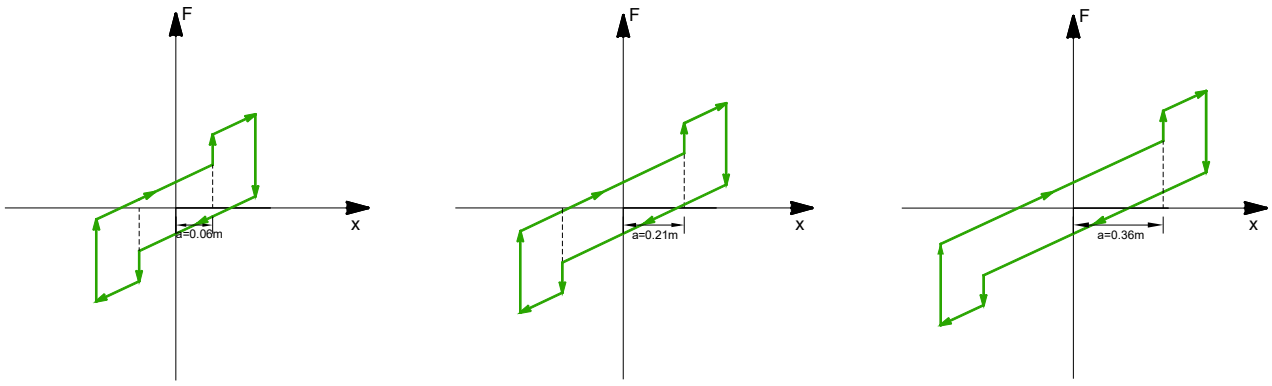

(a) a = 0.06 (Case I-1) (b) a = 0.21 (Case I-2) (c) a = 0.36 (Case I-3)

Fig. 9 Hysteresis curves under different initial gaps with λ_1 = 0.03 and λ_2 = 0.04 (Case I)

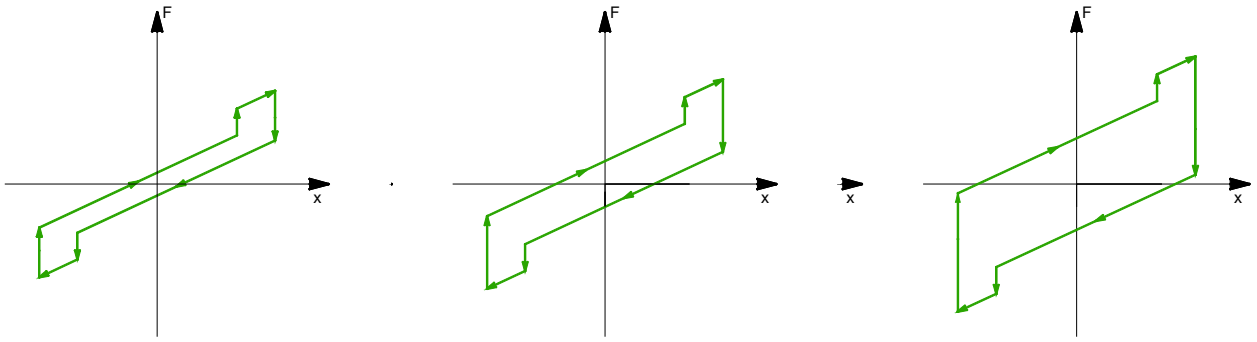

(a) λ_1 = 0.035 (Case II-1) (b) λ_1 = 0.04 (Case II-2) (c) λ_1 = 0.045 (Case II-3)

Fig. 10 Hysteresis curves under different λ_1 of isolator and a = 0.06 m and λ_2 = 0.04 (Case II)

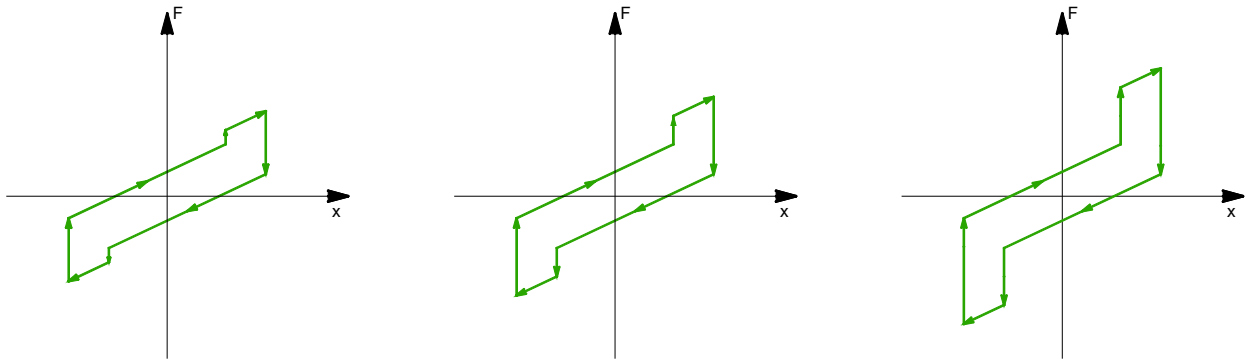

(a) λ_2 = 0.045 (Case III-1) (b) λ_2 = 0.05 (Case III-2) (c) λ_2 = 0.055 (Case III-3)

Fig. 11 Hysteresis curves under different λ_2 of gap damper and a = 0.06 m and λ_1 = 0.065 (Case III)

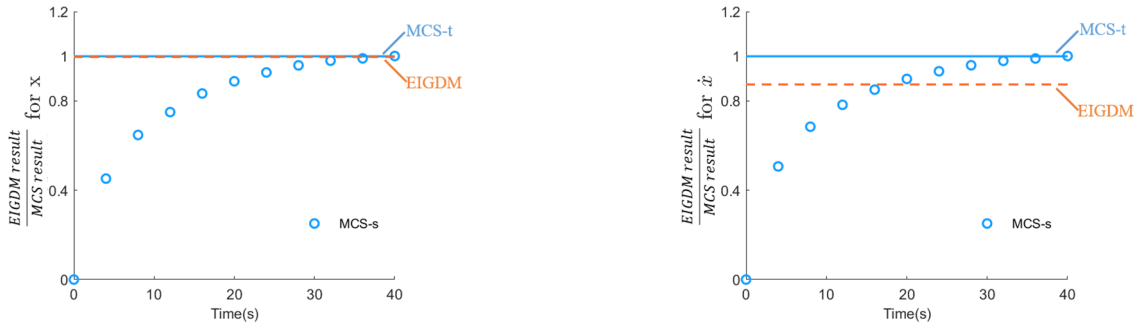

Fig. 12 Error in RMS responses (the initial gap is 0.06) (in m and s)

Fig. 13 Error in RMS responses (the initial gap is 0.21) (in m and s)

Fig. 14 Error in RMS responses (the initial gap is 0.36) (in m and s)

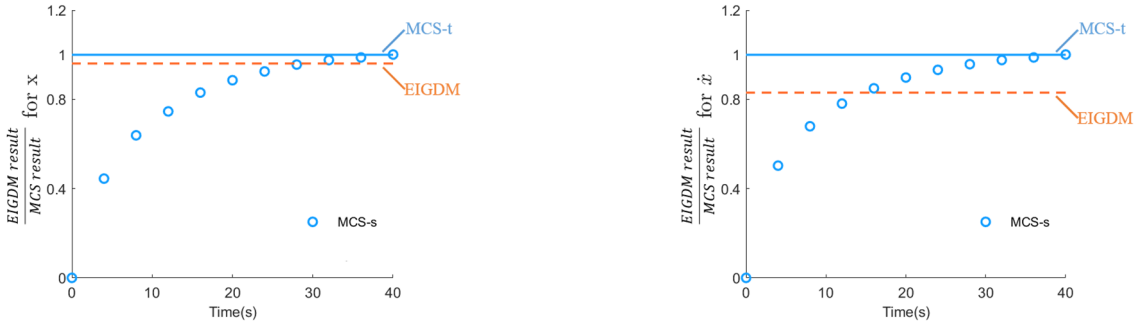

Fig. 15 Error in RMS responses (λ_1 = 0.035) (in m and s)

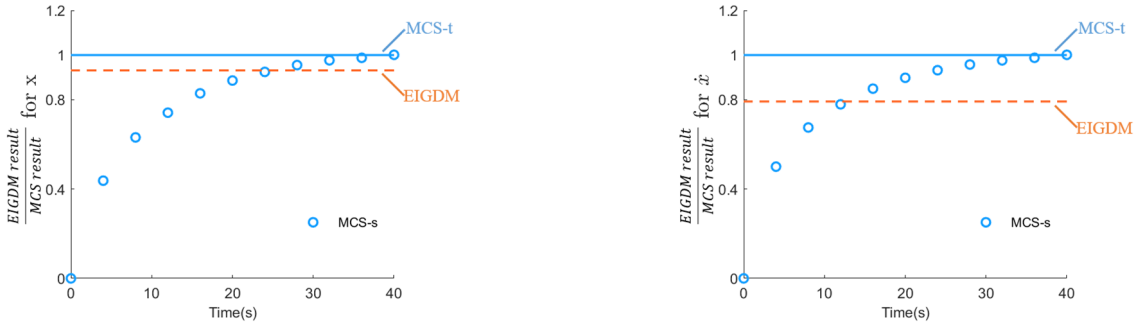

Fig. 16 Error in RMS responses (λ_1 = 0.04) (in m and s)

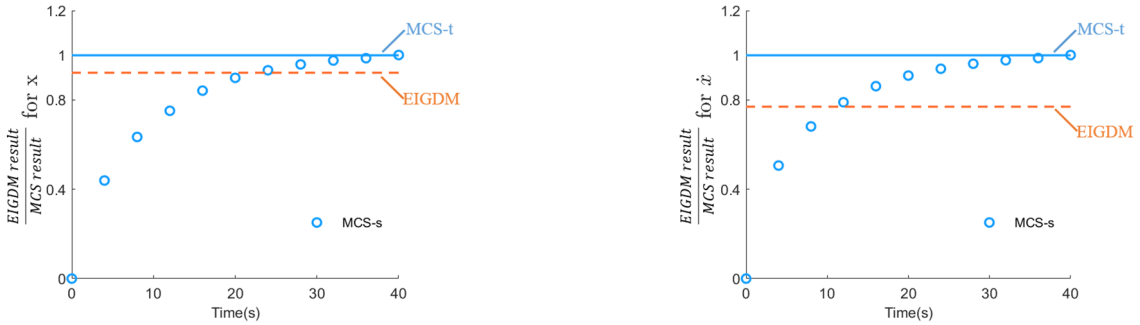

Fig. 17 Error in RMS responses (λ_1 = 0.045) (in m and s)

which can be observed from Figs. 12-14. The errors of σ_x and $\sigma_{\dot{x}}$ between the calculation results of the EIGDM using the Lyapunov equation and the MCS simulation result are less than 10% and 20%, respectively. Particularly when the initial gap is 0.06, the error of σ_x is only 0.2% and $\sigma_{\dot{x}}$ is 13%.

4.2 Different energy consumption coefficients of isolator

As previously mentioned, λ_1 reflects the energy dissipation capacity of the isolator. The parameters involved in Figs. 15-17 are: λ_1 = 0.035, 0.04, and 0.045, whereas a

= 0.06 m and λ_2 = 0.04. The initial gap a of 0.06 m is roughly equal to a distance of 0.6 D_{MCE}, where D_{MCE} is maximum displacement response, as mentioned by Zargar (2013, 2017). Figs. 15-17 show the comparisons of the results of the responses by the equivalent linearization and those by the MCS under different λ_1. The results show that the equivalent linearization gave fairly good results compared with those of the MCS. The error of σ_x is about 10%, and the error of $\sigma_{\dot{x}}$ increases with the increase of energy consumption coefficient of the isolator, which is within 23%.

4.3 Different energy consumption coefficients of gap damper

The parameter λ_2 represents the energy dissipation capacity of the gap damper. The IGD parameters involved in Figs. 18-20 are: a = 0.06 m; λ_1 = 0.065; whereas λ_2 = 0.045, 0.05, and 0.055. In these cases, the errors of $\sigma_{\dot{x}}$ decrease with the increase of energy consumption coefficient of the gap damper. The maximum error is 26% when $\lambda_2 = 0.045$. Simultaneously, the errors of σ_x are within 17% for the three cases.

4.4 Discussion

From the above results of the three groups of cases with different IGD parameters, it can be concluded that the proposed EIGDM incorporating the Lyapunov equation can give reasonable estimation of the nonlinear structural responses under random earthquake excitations compared with the results from the MCS analysis.

The errors of displacement σ_x are increased when the initial gap increases from 0.06 m to 0.36 m, and the energy consumption coefficients of isolator λ_1 increase from 0.035 to 0.045, and λ_2 is 0.04, which are within 10% in those cases. Simultaneously, the errors of $\sigma_{\dot{x}}$ increase from 13% to 23%. The errors of σ_x and $\sigma_{\dot{x}}$ increase and reduce

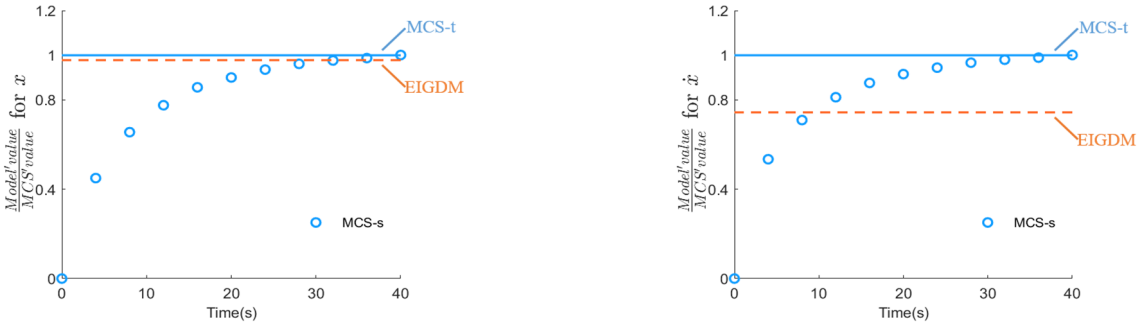

Fig. 18 Error in RMS responses (λ_2 = 0.045) (in m and s)

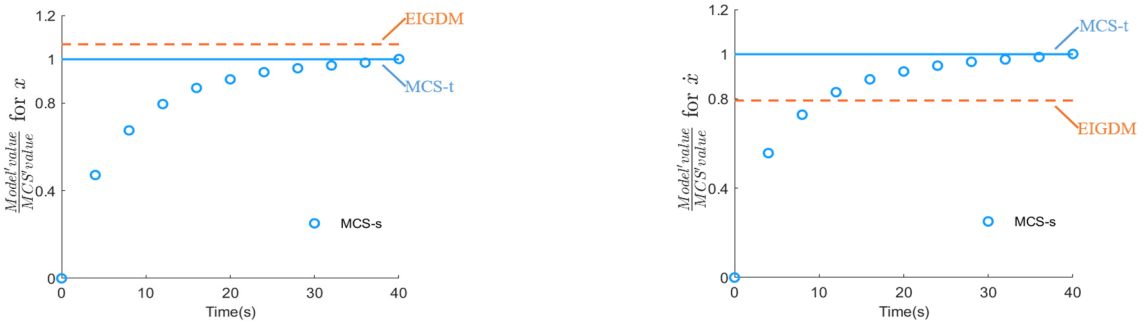

Fig. 19 Error in RMS responses (λ_2 = 0.05) (in m and s)

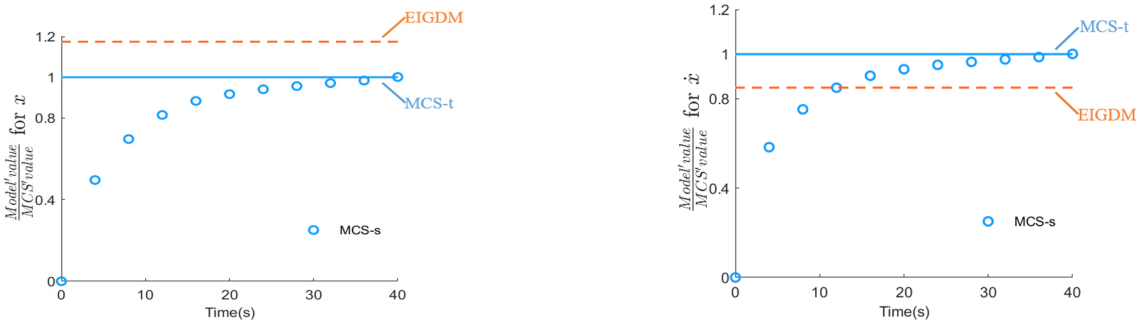

Fig. 20 Error in RMS responses (λ_2 = 0.055) (in m and s)

separately, when the energy consumption coefficients of the gap damper increase from 0.045 to 0.055, and the initial gap is 0.06, λ_1 is 0.065. And the maximum error of σ_x and $\sigma_{\dot{x}}$ is 17% and 26%.

To sum up, both the error of σ_x and $\sigma_{\dot{x}}$ can be controlled within 23%, except the case when λ_1 is 0.065, λ_2 is 0.045 and the gap is 0.06. Moreover, when the energy consumption coefficient λ_1 and λ_2 are relatively small, the IGDM is controlled by displacement, so the errors of σ_x are smaller than the errors of $\sigma_{\dot{x}}$. In terms of isolator, the error of the IGDM increases when the nonlinearity of isolator increases, corresponding to increased λ_1. On the other hand, larger energy consumption coefficient of isolator and damper result in better earthquake energy dissipation capacity, then choose an optimized parameter group is a task of engineers.

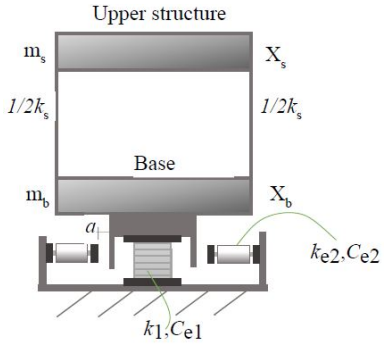

Fig. 21 Model with a SDOF structure and an IGD

5. Verification on a structure with an IGD

In the previous section, the feasibility of the equivalent linearized IGDM (EIGDM) was verified for a rigid structure with an IGD. In this section, a structure with a single degree of freedom (SDOF) is considered, which consists of an upper structure and a base as in Fig. 21 to investigate the effect of the IGD on the structure. The structural parameters are taken as: $m_s = 250 \times 10^2\ kg$, $m_b = 230 \times 10^2$ kg, $k_s = 3000$ kN/m, and damping ratio $\xi = 2\%$. Then the natural frequency and period of the structure without the IGD are 1.75 Hz and 0.57 s. Using the proposed EIGDM, the responses of the upper structure and base were analyzed under two levels of earthquake with the exceedance probabilities of 10% in 50 and 100 years in Los Angeles (Level 1 and Level 2), which were considered as different intensity for earthquake design. The parameters of the IGD are: $k_1 = 600$ kN/m, the initial gap a = 0.36 m, and the energy dissipation coefficients $\lambda_1 = 0.065$ and $\lambda_2 = 0.05$ at both earthquake levels. The natural frequency and period of the structure with the IGD are: 0.55 Hz and 1.83 s, respectively. The above parameters are defined referring to the structural character in literature (Zargar *et al*. 2017). The parameters of the K-T spectrum for Level 1 were shown in Section 4, while those for Level 2 were taken as: $S_0 = 0.052\ m^2/s^2$, $\omega_g = 4.9\ rad/s$ and $\xi_g = 1.76$. In the MCS, 10000 earthquake waves were generated from the K-T model with the same site parameters used in Section 4. Figs. 22 and 23 show the RMS responses of the upper structure and base obtained from the MCS at the two levels of earthquake with varying number of earthquake waves. The results indicate that about 10000 simulated earthquake waves are needed to obtain converging

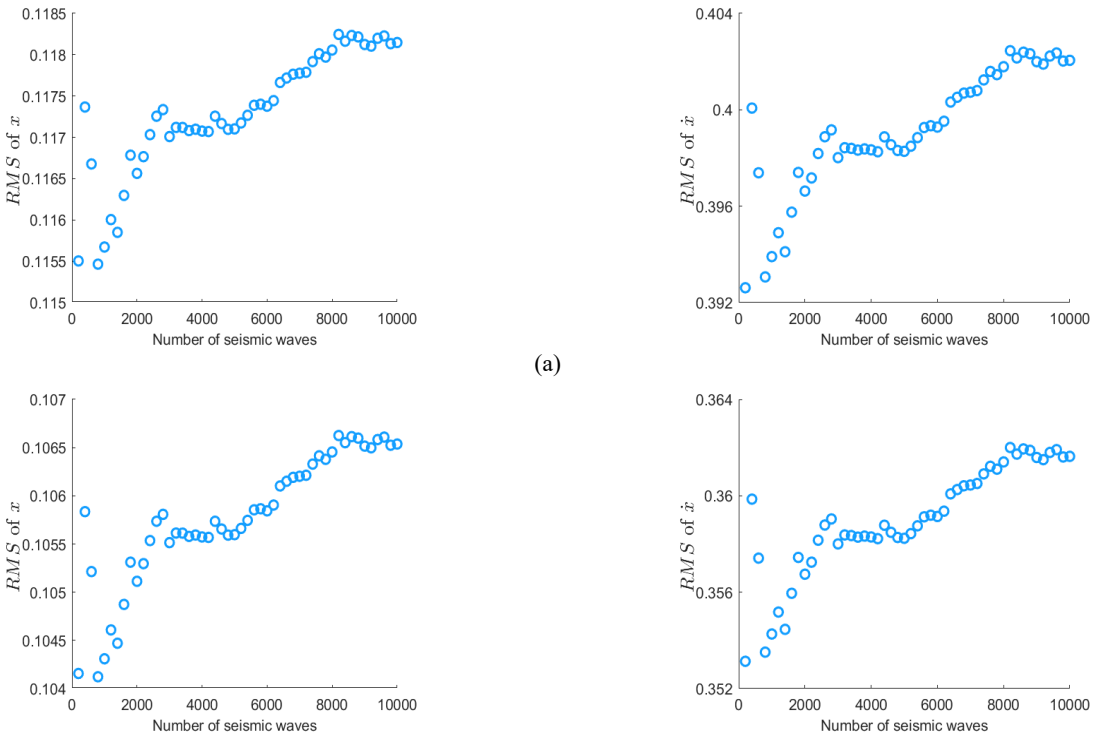

Fig. 22 RMS responses for different numbers of earthquake waves at Level 1: (a) upper structure; (b) base

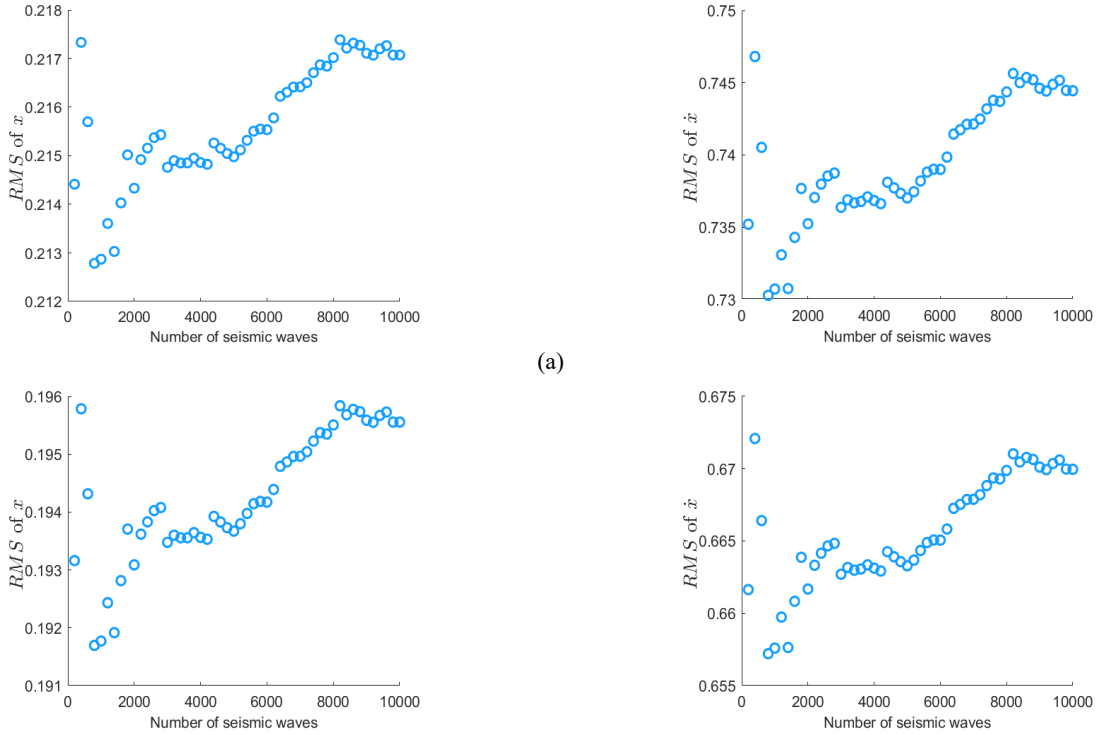

Fig. 23 RMS responses for different numbers of earthquake waves at Level 2: (a) upper structure; (b) base

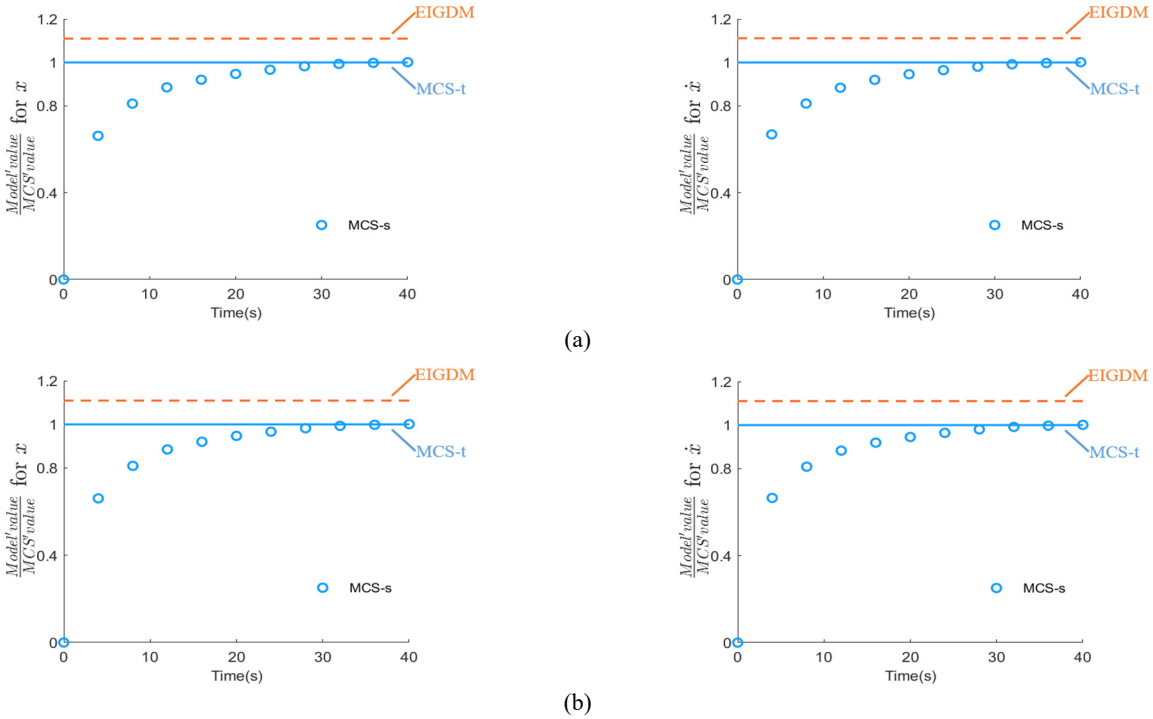

Fig. 24 Error in RMS responses for earthquake of Level 1: (a) upper structure; (b) base

responses with a constant of 0.001 in the relative error, which requires huge computational efforts in the nonlinear dynamic analysis of large- structures for the simulated ground excitations. Figs. 24 and 25 show the ratios of the RMS responses attained by the EIGDM and MCS. The results of the EIGDM show fairly good agreement with those of the MCS analysis (MCS-t). As demonstrated, the errors in σ_x and $\sigma_{\dot{x}}$ of the upper structure are about 11% and 18% for earthquake responses of Level 1 and 2, respectively.

The performance of the IGD was investigated using the results of the EIGDM in comparison with those without the

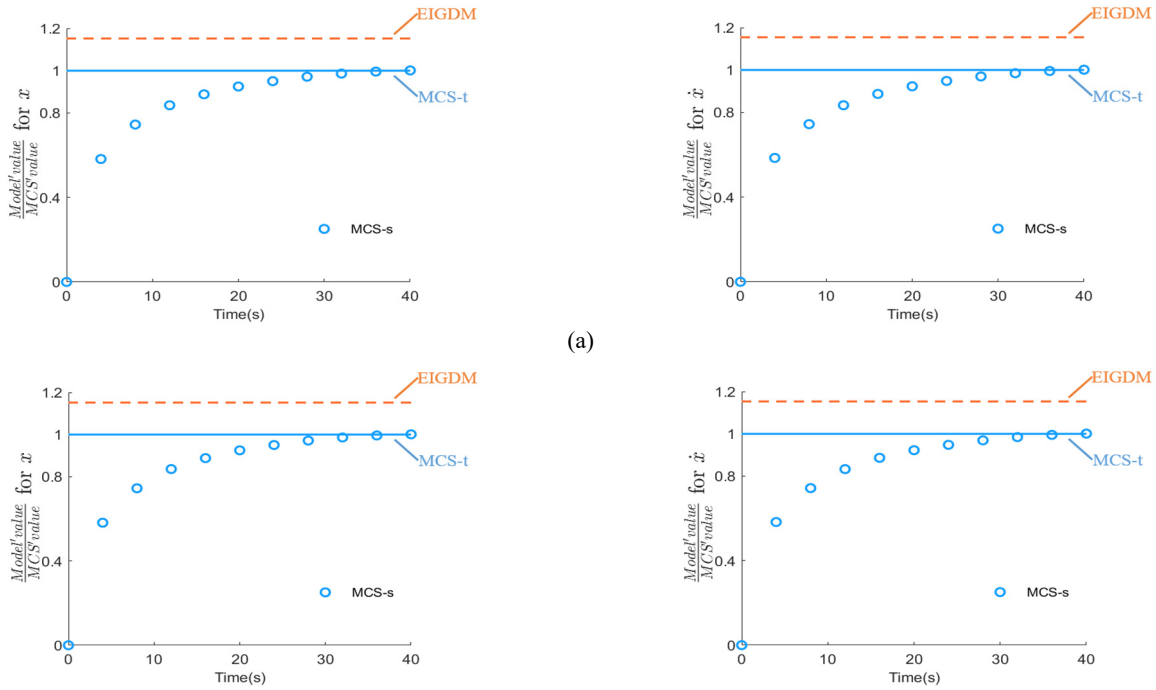

(a)

(b)

Fig. 25 Error in RMS responses for earthquake of Level 2: (a) upper structure; (b) base

IGD. The covariance matrix was obtained by Lyapunov equation for the structure with the IGDM at Level 1 earthquake as in Table 2, from which the RMS of the upper structure and base with IGD system were obtained as 0.128 and 0.115 m, respectively. On the other hand, the RMS of the upper structure without the IGD was obtained as 0.117 m. Table 3 shows the covariance matrix for the structural responses with the IGDM at earthquake of Level 2.

The RMS of the relative displacement of the upper structure can be computed from the covariance matrix as

$$\text{RMS } X_s^r = \sqrt{\sigma_{xs,xs}^2 + \sigma_{xb,xb}^2 - 2cov(X_s, X_b)} \qquad (15)$$

Where $cov(X_s, X_b)$ is the covariance of X_s and X_b. From Table 2, RMS X_s^r was obtained as 0.01 m and 0.047 m for the cases with and without IGD under earthquake of Level 1. RMS X_s^r was obtained as 0.024 m and 0.065 m for the cases with and without IGD under earthquake of Level 2 from Table 3.

Finally, the RMS of the member force F_s was obtained as

$$\text{RMS } F_s = k_s * \text{RMS } X_s^r \qquad (16)$$

where they were obtained as 30 kN and 141 kN for cases with and without the IGD at earthquake of Level 1, and 72 kN and 195 kN for at earthquake of Level 2. The above results indicate that the RMS of the member force of the upper structure is reduced significantly to the level of 21% and 37% of that without the IGD for the two levels of earthquake cases.

The RMS of the base displacement was found as 0.115 m and 0.219 m for earthquake cases of Level 1 and 2, from which the maximum base motion was approximate to 0.345 m and 0.658 m using a peak factor of 3 (Clough and Penzien 1995). This maximum value is found to be larger than the gap (0.36 m) particularly for Level 2 earthquake, which indicates the full of utilization the IGD elements (isolator and gap damper).

As stated above, the proposed EIGDM is provided as a simple and effective method to estimate the nonlinear responses of structures with an IGD for random earthquake excitations for different earthquake intensity. With this method, large amount of computation work for the MCS can be avoid and instead by solving the Lyapunov equation corresponding to the EIGDM, which demonstrates great computational efficiency and adaptability to the seismic design of structures with IGD system.

Table 2 Covariance matrix of the structural response with IGD for earthquake of Level 1 (in m)

Cov.	X_s	X_b	$\dot{X}_s$	$\dot{X}_b$
X_s	0.0164	0.0148	0.0000	0.0007
X_b	0.0148	0.0133	-0.0007	0.0000
$\dot{X}_s$	0.0000	-0.0007	0.1904	0.1709
$\dot{X}_b$	0.0007	0.0000	0.1709	0.1538

Table 3 Covariance matrix of the structural response with IGD for earthquake of Level 2 (in m)

Cov.	X_s	X_b	$\dot{X}_s$	$\dot{X}_b$
X_s	0.0593	0.0534	0.0000	0.0013
X_b	0.0534	0.0481	-0.0013	0.0000
$\dot{X}_s$	0.0000	-0.0013	0.7002	0.6293
$\dot{X}_b$	0.0013	0.0000	0.6293	0.5663

6. Conclusions

The isolator-gap damper (IGD) system was analyzed via the proposed mathematical interpretation for the nonlinear hysteretic behavior and its equivalent linearization method (EIGDM). Nine different parameters including the initial gap and energy dissipation coefficients were analyzed for a rigid structure to verify the accuracy of the EIGDM. Then a SDOF structure was analyzed using the proposed EIGDM to investigate the effectiveness of the IGD in reduction of the earthquake responses of the structure. Finally, the following conclusions have been drawn.

(1) A mathematical hysteretic model to describe the nonlinear characteristics of the IGD system is represented using three separated models, and it had been successfully applied to the time history analysis using simulated earthquakes by the MCS.
(2) The proposed EIGDM was verified for various cases with different initial gap and energy dissipation coefficients using the Lyapunov equation. The difference (error) of the displacement in the RMS responses between the EIGDM and MCS results were less than 17% which indicates the adequacy of the proposed method.
(3) The analysis for a SDOF structure with an IGD also verified the feasibility of the EIGDM with good agreement to the MCS results. The errors in the RMS structural responses were about 11% and 17% for earthquake with the exceedance probabilities of 10% in 50 and 100 years.
(4) The RMS of the structural responses with the IGD indicates the effectiveness of the IGD in reducing the member force for the earthquake excitations. The responses reduced to 21% and 37% of the one without an IGD for the two earthquake levels.

In this study, it was assumed that the seismic process is a stationary Gaussian process and the response analysis was carried out on an idealized SDOF structure. Future works may be focused on special excitation processes, such as nonstationary and site specific excitations, and responses of multi-degree-of-freedom structures with an IGD device of various kinds, and the design optimization of the IGD system using the EIGDM.

Acknowledgments

The research described in this paper was financially supported by the National Key R&D Program of China (2019YFE0112600), the National Natural Science Foundation of China (Grant Nos. 52078459) and the National Natural Science Foundation of Zhejiang Province (Grant Nos. LZ22E080005).

References

Clough, R.W. and Penzien, J. (1995), *Dynamics of Structures*, (Third Edition), Computers & Structures, Inc., USA.

Crandall, S.H. and Mark, W.D. (1963), *Random Vibration in Mechanical Systems*, New York Academic Press.

Dickinson, B. and Gavin, H. (2010), "Parametric statistical generalization of uniform-hazard earthquake ground motion", *J. Struct. Eng.*, **137**(3), 410-422. https://doi.org/10.1061/(ASCE)ST.1943-541X.0000330

De Domenico, D., Gandelli, E. and Quaglini, V. (2020a), "Effective base isolation combining low-friction curved surface sliders and hysteretic gap dampers", *Soil Dyn. Earthq. Eng.*, **130**, 105989. https://doi.org/10.1016/j.soildyn.2019.105989

De Domenico, D.D., Gandelli, E. and Quaglini, V. (2020b), "Adaptive isolation system combining low-friction sliding pendulum bearings and SMA-based gap dampers", *Eng. Struct.*, **212**, 110536. https://doi.org/10.1016/j.engstruct.2020.110536

Farsangi, E.N., Tasnimi, A.A. and Yang, T.Y. (2018), "Seismic performance of a resilient low-damage base isolation system under combined vertical and horizontal excitations", *Smart Struct. Syst., Int. J.*, **22**(4), 383-397. https://doi.org/10.12989/sss.2018.22.4.383

Gazi, H. and Alhan, C. (2018), "Probabilistic sensitivity of base-isolated buildings to uncertainties", *Smart Struct. Syst., Int. J.*, **22**(4), 441-457. https://doi.org/10.12989/sss.2018.22.4.441

Han, M. and Wang, X.M. (2005), "Experimental study on soft pounding limiting deformation of base isolating layer", *Earthq. Resist. Eng. Retrofit.*, **27**(03), 70-729.

Han, M., Li, X.H. and Du, H.K. (2007), "Experiment on limiting displacement of steel spiral spring soft-collision for a base isolating layer", *World Earthq. Eng.*, **23**(04), 39-43.

Han, M., Du, H.K. and Li, X.H. (2008), "Testing study on soft-collision limiting displacement of base isolating layer", *Eng. Mech.*, **25**(S1), 124-128.

Kanai, K. (1957), "Semi-empirical formula for the seismic characteristics of the ground", Earthquake Research Institute, University of Tokyo, Japan.

Kelly, J.M. (1999), "The role of damping in seismic isolation", *Earthq. Eng. Struct. Dyn.*, **28**(1), 3-20. https://doi.org/10.1002/(SICI)1096-9845(199901)28:1<3::AID-EQE801>3.0.CO;2-D

Kishida, A., Nishimura, N., Yamashita, Y., Taga, K., Fujitani, H. and Mukai, Y. (2017), "Response reduction methods for base isolated buildings with collision to retaining walls", In: *Sensors and Smart Structures Technologies for Civil, Mechanical, and Aerospace Systems 2017*. https://doi.org/10.1117/12.2256229

Lei, Z. and Qiu, C. (1997), "An equivalent nonlinearization method for analysing response of nonlinear systems to random excitations", *Appl. Mathe. Mech.*, **18**, 551-561. https://doi.org/10.1007/BF02454114

Li, Y. and Li, J. (2019), "Overview of the development of smart base isolation system featuring magnetorheological elastomer", *Smart Struct. Syst., Int. J.*, **24**(1), 37-52. https://doi.org/10.12989/sss.2019.24.1.037

Liu, C., Huang, H.Y. and Xiong, Z.M. (2018), "Research on new limiting device for pure friction base-isolated structure", *Earthq. Resist. Eng. Retrofit.*, **40**(06), 74-80.

Nakashima, M. and Bruneau, M. (1995), *Preliminary Reconnaissance Report of the 1995 Hyogoken-Nanbu Earthquake*, The Architectural Institute of Japan, April.

Ou, J.P. and Wang, G.Y. (1998), *Random Vibration of Structures*, Higher Education Press, Beijing, China.

Pan, P., Zamfirescu, D., Nakashima, M., Nariaki, N. and Kashiwa, H. (2005), "Base-isolation design practice in Japan: introduction to the post-Kobe approach", *J. Earthq. Eng.*, **9**(1), 147-171.

Rawlinson, T., Marshall, J., Ryan, K. and Zargar, H. (2015), "Development and experimental evaluation of a passive gap damper device to prevent pounding in base-isolated structures", *Earthq. Eng. Struct. Dyn.*, **44**, 1661-1675. https://doi.org/10.1002/eqe.2542

Roberts, J.B. (1981a), "Response of nonlinear mechanical systems to random excitation part 1", *Shock Vib. Digest*, **13**, 15-28.
Roberts, J.B. (1981b), "Response of nonlinear mechanical systems to random excitation part 2", *Shock Vib. Digest*, **13**, 13-29.
Ryan, K., Zargar, H., Marshall, J. and Rawlinson, T. (2016), "Experimental Validation of a Gap Damper to Control the Displacement Demands in a Seismically Isolated Building", *Proceedings of the 16th World Conference on Earthquake Engineering*, Santiago, Chile, January.
Sato, E., Furukawa, S., Kakehi, A. and Nakashima, M. (2011), "Full-scale shaking table test for examination of safety and functionality of base-isolated medical facilities", *Earthq. Eng. Struct. Dyn.*, **40**, 1435-1453. https://doi.org/10.1002/eqe.1097
Somerville, P., Smith, N., Punyamurthula, S. and Sun, J. (1997), "Development of ground-motion time histories for phase 2 of the FEMA/SAC steel project", Rep. No. SAC/BD-97/04, FEMA, Washington, DC, USA.
Soong, T.T. and Grigoriu, M. (1993), "Random vibration of mechanical and structural systems", NASA STI/Recon Technical Report A, 93, p. 14690.
Tremblay, R., Lacerte, M. and Christopoulos, C. (2008), "Seismic response of multistory buildings with self-centering energy dissipative steel braces", *J Struct Eng.*, **134**(1), 108-20.
Tu, J., Lin, P., Stoten, D.P. and Guang, Li. (2009), "Testing of dynamically substructured, base-isolated systems using adaptive control techniques", *Earthq. Eng. Struct. Dyn.*, **39**, 661-681. https://doi.org/10.1002/eqe.962
Yan, X. and Nie, J. (2000), "Response of SMA superelastic systems under random excitation", *J. Sound Vib.*, **238**(5), 893-901. https://doi.org/10.1006/jsvi.2000.3020
Xiong, Z.M., Huo, X.P. and Su, N.N. (2008), "Theoretical analysis of a new kind of sliding base isolation frame structure", *J. Vib. Shock*, **27**(10), 124-129.
Xu, J., Spencer, B. and Lu, X. (2017), "Performance-based optimization of nonlinear structures subject to stochastic dynamic loading", *Eng. Struct.*, **134**, 334-345. https://doi.org/10.1016/j.engstruct.2016.12.051
Xu, J., Fermandois, G.A., Spencer, B. and Lu, X. (2018), "Stochastic optimization of buckling restrained braced frames under seismic loading", *Struct. Infrastr. Eng.*, **14**, 1386-1401. https://doi.org/10.1080/15732479.2018.1443144
Yang, C., Chen, Y.Y., Liao, W.L., Luo, L. and Wu, D.C. (2019), "Collisions behaviors analysis of base-isolation building structures based on the elastoplastic model of horizontal stop blocks", *J. Build. Struct.*, 1-10[2021-04 05]. https://doi.org/10.14006/j.jzjgxb.2019.0802
Zargar, H., Ryan, K. and Marshall, J. (2013), "Feasibility study of a gap damper to control seismic isolator displacements in extreme earthquakes", *Struct. Control Health Monitor.*, **20**(8), 1159-1175. https://doi.org/10.1002/stc.1525
Zargar, H., Ryan, K., Rawlinson, T. and Marshall, J. (2017), "Evaluation of a passive gap damper to control displacements in a shaking test of a seismically isolated three-story frame", *Earthq. Eng. Struct. Dyn.*, **46**, 51-71. https://doi.org/10.1002/eqe.2771
Zhang, H.M., Quan, L.M., Lu, X.L. and Xu, J.Q. (2020), "Modified flag-shaped model for self-centering system and its equivalent linearization and structural optimization for stochastic excitation", *Eng. Struct.*, **215**, 110420. https://doi.org/10.1016/j.engstruct.2020.110420
Zhang, H.M., Quan, L.M., Lu, X.L. (2022), "Experimental hysteretic behavior and application of an assembled self-centering buckling-restrained brace", *J. Struct. Eng.-ASCE*. https://doi.org/10.1061/(ASCE)ST.1943-541X.0003287
Zhao, G.F., Ma, Y.H. and Zhang, Y.S. (2013), "Analysis on parameters of hysteretic-friction isolated system with elastic-plastic displacement-constraint device", *J. Build. Struct.*, **34**(01), 131-138.

HJ